Available online at www.sciencedirect.com
SCIENCE DIRECT®
Mechanical Systems and Signal Processing 20 (2006) 953–965
Mechanical Systems and Signal Processing
www.elsevier.com/locate/jnlabr/ymssp

A current monitoring system for diagnosing electrical failures in induction motors

G.G. Acosta*, C.J. Verucchi, E.R. Gelso

Department of Electromechanics, Facultad de Ingeniería–UNCPBA, Av. Del Valle, 5737, B7400JWI Olavarria, Buenos Aires, Grupo INTELYMEC, Argentina

Received 24 April 2004; received in revised form 19 August 2004; accepted 3 October 2004
Available online 23 November 2004

Abstract

Induction motors are critical components in industrial processes. A motor failure may yield an unexpected interruption at the industrial plant, with consequences in costs, product quality, and safety. Many of these faulty situations in three phase induction motors have an electrical reason. Among different detection approaches proposed in the literature, those based on stator current monitoring are advantageous due to its non-invasive properties. One of these techniques resorts to spectrum analysis of machine line current. Another non-invasive technique is the Extended Park's Vector Approach, which allows the detection of inter-turn short circuits in the stator winding. This article presents the development of an on-line current monitoring system that uses both techniques for fault detection and diagnosis in the stator and in the rotor. Based on experimental observations and on the knowledge of the electrical machine, a knowledge-based system was constructed in order to carry out the diagnosis task from these estimated data.

Keywords: Fault diagnosis; Induction motor; Current monitoring

*Corresponding author. Tel.: +54 2284 4510655; fax: +54 2284 4506628.
E-mail addresses: gerardo.acosta@ieee.org, ggacosta@fio.unicen.edu.ar (G.G. Acosta), verucchi@fio.unicen.edu.ar (C.J. Verucchi), egelso@fio.unicen.edu.ar (E.R. Gelso).

0888-3270/$ - see front matter
doi:10.1016/j.ymssp.2004.10.001

1. Introduction

Induction motors are essential components in the vast majority of industrial processes. The different faults on induction machines may yield drastic consequences for an industrial process. The main problems are related to increasing costs, and worsening of process safety conditions and final product quality. Many of these faults show themselves gradually. Then the detection of incipient faults allows avoiding unexpected factory stops and saving a great deal of money [1,2]. The kind of faults of these machines are varied. However the most frequent are [3]:

(a) opening or shorting of one or more of a stator phase winding,
(b) broken rotor bar or cracked rotor end-rings,
(c) static or dynamic air-gap irregularities, and
(d) bearing failures.

These faults may be observed through some of the following symptoms [4]:

(a) unbalanced air-gap voltages and line currents,
(b) increased torque pulsations,
(c) decreased average torque,
(d) increased losses and
(e) excessive heating.

The reason for such faults may reside in small errors during motor manufacturing, improper use, high level of requirements in motor start-up, ventilation deficiency, and others. Motors actuated by pulse width modulation (PWM) voltage source inverters, have greater probabilities to fail in their bearings [5] and in their stator windings' insulation [6].

Several diagnosis techniques for the identification and discrimination of the enumerated faults have been proposed. Temperature measurements, infrared recognition, radio frequency emissions, noise monitoring or chemical analysis are some of them [4]. References for coils to monitor the motor axial flux may be found in [7], vibration measurement, in [8,9]. Spectrum analysis of machine line current (called motor current signature analysis or MCSA) is referred to in [10,11], Park's Vector currents (PVC) Monitoring, in [12,13], artificial intelligence based techniques are used in [14–16].

From all these approaches proposed in the literature, those based on stator current monitoring are advantageous because of its non-invasive feature. One of these techniques is the MCSA, in which rotor faults become apparent by harmonic components around the supply frequency. The amplitude of these lateral bands allows dimensioning the failure's degree [4]. Also, the Extended Park's Vector Approach (EPVA), based on the observation of the Park's complex vector module, allows the detection of inter-turn short circuits in the stator winding. This article presents the development of an on-line current monitoring system (CMS) to perform the diagnosis task in a supervisory system [17]. This last task employs both techniques (MCSA and EPVA) in an integrated way, for fault detection and diagnosis in the stator and in the rotor of an induction motor, respectively. The selection of both techniques, due to MCSA as well as EPVA, shares the stator current sensing, and then the same information may be used as input for both methods. In this way, current spectral components convey information about the rotor state, while the EPVA

is appropriate for the stator windings monitoring, as it will be shown. The proposed CMS uses a National^{TM} data acquisition equipment and is programmed in LabView^{TM}. From the acquired current data and the motor features, the CMS estimates the slip and load percentage. Based on experimental observations and on the knowledge of the electrical machine, a knowledge-based system (KBS) was constructed in order to carry out the diagnosis task from these estimated data. The results of each diagnosis are outcomes in the CMS screen in the form of fault modes index. If necessary, a warning is given to put the motor under new observations (i.e. to measure the rotor speed or to change the motor load), or even to verify the power distribution net balance. Experimental results are presented from an induction motor of 380 V, 7.5 HP and 1000 rpm, especially designed for running under different failure circumstances. These results with a high degree of correct diagnosis show a right direction to explore.

2. Fault detection from stator currents

2.1. Motor current signature analysis

When there are broken or even fissured bars, the rotor's impedance exhibits an unbalance. The immediate consequence of such an unbalance is the existence of inverse sequence currents. These currents have a frequency that is equal to the product of the slip (s) and the supply frequency (f). They generate a magnetic field that turns counter motor rotation-wise. This magnetic field is called inverse magnetic field or IMF. The speed of this IMF is given by the expression (1):

$$\omega_i^r = -s\omega_s, \tag{1}$$

where ω_i^r is the speed of IMF, s the slip and ω_s the angular supply frequency.

If translated to stationary co-ordinates, such a speed may be re-written as

$$\omega_i^s = -s\omega_s + \omega_r = (1 - 2s)\omega_s, \tag{2}$$

where ω_r is the rotor speed.

The amplitude of IMF depends on two features. The first is the unbalance degree in the rotor circuit (number of broken bars), and the second is the value of the current in the rotor bars. This last depends on the motor's load state. In this way, the IMF originated in the rotor's impedance unbalance produce harmonic currents of frequency $(1-2s)f$ in the stator windings. These currents interact with the main magnetic field and set a torque over the rotor, which oscillates with a frequency of $2sf$ [18]. This pulsating torque provokes an oscillation also in the rotor speed. The amplitude of this oscillation is a function of the motor's load inertia. As a reaction of such speed perturbation, new currents arise in the stator at a frequency $(1 \pm 2s)f$. The new current component at frequency $(1–2s)f$ is superimposed with the original, and then modifies its amplitude. In this way, it is concluded that rotor faults in an induction motor, can be determined from the observation of the sidebands in the stator current spectrum, in the neighbourhood of both frequencies given by

$$f_{SB} = (1 \pm 2s)f. \tag{3}$$

An example of the current spectrum of a motor with this fault is shown in Fig. 1.

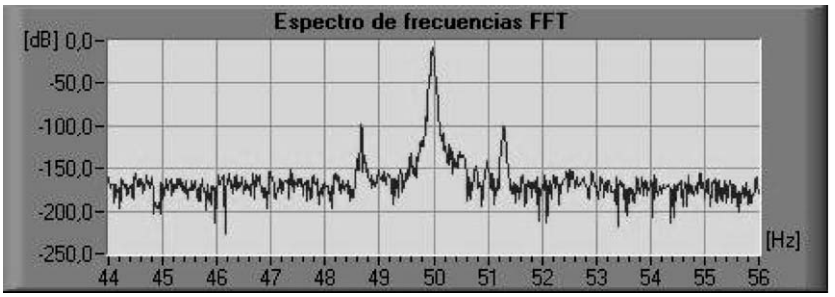

Fig. 1. Frequency spectrum of one phase stator current of a motor with three broken bars and full load.

As regards the amplitude of these stator current sidebands, they depend on three factors: the motor's load inertia, the motor's load torque, and the severity of the fault. So, the first two factors must be suppressed in order to analyse, as independently as possible, the one of concern for the present application.

The motor's load inertia can be avoided if the sum of both sidebands component are considered, as proposed in [18]. As regards the motor's load torque, there is always a relationship between the amplitude of the sidebands and the amplitude of the fundamental component of the stator current at the supply frequency. Then, working with normalised amplitude values as regards this supply frequency component, allows to partially avoid the influence of this second factor. However, side bands reveal faults more clearly with high values of slip. Then it is recommended that the diagnosis were carried out with the motor running near its nominal load.

Then, a severity factor can be defined as

$$S_{RF} = \frac{I_{(1\pm 2s)f}}{I_1} 100, \tag{4}$$

where S_{RF} is the severity rotor fault, $I_{(1\pm 2s)f}$ is the sum of amplitude of sidebands, and I_1 is the amplitude of the fundamental component of the stator current.

2.2. Extended Park's Vector Approach

The Park's transform [19], allows the representation of the variables of a three phases machine through a co-ordinates system with two perpendicular axes. The components of the stator currents in the direct and quadrature axes (D and Q) are computed by means of the following expressions:

$$i_D = \sqrt{\frac{2}{3}} i_A - \sqrt{\frac{1}{6}} i_B - \sqrt{\frac{1}{6}} i_C, \tag{5}$$

$$i_Q = \sqrt{\frac{1}{2}} i_B - \sqrt{\frac{1}{2}} i_C, \tag{6}$$

where i_A, i_B and i_C are the stator currents. Under ideal conditions, that is, when a normal behaviour motor is fed with a sinusoidal, balanced and positive sequence three-phases current

system, the Park's components or Park's Currents Vector (PVC) results in

$$i_D = \frac{\sqrt{6}}{2} I_{\max} \sin(\omega_s t), \tag{7}$$

$$i_Q = \frac{\sqrt{6}}{2} I_{\max} \sin(\omega_s t - \pi/2). \tag{8}$$

In this expression $I_{\max}$ is the maximum stator current value and t is the time variable. Eqs. (7) and (8) describe a perfect circle centred in the origin of the plane D–Q, with constant radius equal to $(\sqrt{6}/2)$. Fig. 2 presents the PCV from a Lab experiment of an induction motor under normal conditions. The small variations in the vector radius are due to small unbalanced voltages of distribution system. In the same way, the space and slot harmonics introduce small perturbation in the vector radius. They are negligible for the present analysis and are then filtered in the data acquisition stage.

One of the most common faults in induction motors consists of inter-turn short circuits. In this case, the motor behaves like an unbalanced load, and the stator currents are no longer a balanced system. This abnormal behaviour causes an oscillation in the PVC radius, turning the original circle into elliptical shapes, as may be seen in Fig. 3 for a motor with two coils of phase a (over a total of sixteen) in short circuit. The inclination of the ellipse mayor axis shows the phase in which the fault was produced [13].

Cruz and Marquez Cardoso [12] propose to observe the radius of the geometric locus of the PVC along time in order to obtain a fault diagnosis. Effectively, as this radius oscillates between a maximum and a minimum twice in a supply frequency cycle, it may be decomposed in a Fourier's series. This series presents a direct current component plus a component in twice the net frequency (I_{2NF}). This is shown in Fig. 4 in which it is depicted that a motor with stator coil faults. The amplitude of I_{2NF} is again related to the dimension of the fault and then a new severity factor may

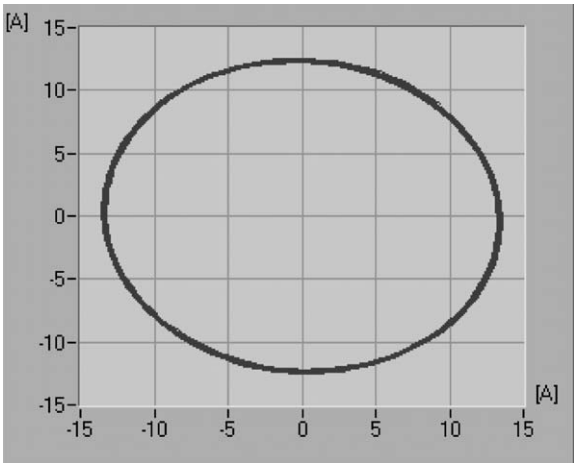

Fig. 2. Geometric locus for the Park's Currents Vector for a motor with normal behaviour.

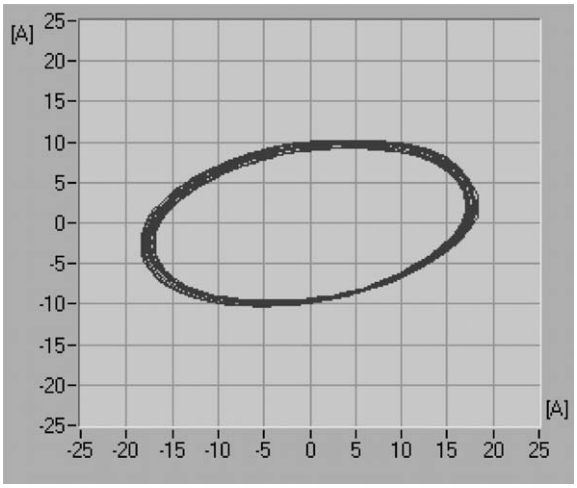

Fig. 3. Geometric locus for the Park's Currents Vector for a motor with coils in shortcut.

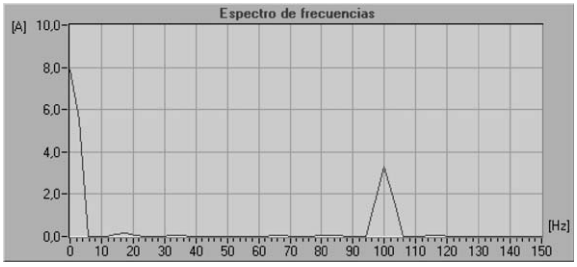

Fig. 4. Harmonic analysis of the Park's Vector module.

be defined as [12]:

$$S_{SF} = \frac{I_{2NF}}{I_{cc}} 100. \tag{9}$$

It is important to take into account that this severity factor varies with motor load, decreasing as the motor approximates to its nominal load.

3. Towards an integrated fault diagnostic system

One aim of the present work was to combine the previous techniques and, in some way, to take the better of them in a single, integrated diagnostic system.

From the stator spectral analysis (MCSA) it is possible to detect rotor as well as stator winding faults, as presented in [20]. However, in the last case, the frequency characterising the fault must

be computed considering the motor poles number, the slip, and the winding features. Also, another handicap of this approach is that it is not possible to relate the fault severity with the amplitude of these frequencies characterising the fault. In contrast, in EPVA the frequency to discriminate a fault is always fixed and twice the supply frequency. Also EPVA only uses the current fundamental component to draw the Park's geometric locus. It is then possible to filter any higher frequency making the procedure more robust in front of noise and perturbations. This is the reason for selecting this last approach for fault detection and diagnosis in the stator.

To obtain a useful diagnosis for the rotor of the induction motor, some authors describe the viability of detecting broken bars by means of the PVC [21]. It is not clear yet that one method is better than the other for this case. However, as the MCSA has been used for so long, giving enough proofs of utility at industrial environments [20], it is the approach selected in this work for detecting and diagnosing rotor electrical faults.

In a normal running, the CMS set the state of the rotor and then the state of the stator winding. It is necessary to determine the frequencies at which harmonic components will appear, because a torque that oscillates may be confused with a fault mode [22]. In order to achieve this, a motor slip is estimated from the no-load current, assuming it is in quadrature with the load component. With both currents a phasorial diagram may be built (as shown in Fig. 5). From the measured stator current (I_S) in Fig. 5, the load component is computed for the present running state. This value is compared to the load component of the nominal current to obtain a motor load index (M_{LI}). Then from M_{LI} and the nominal speed, the motor slip is estimated (S_E), according to the scheme of Fig. 6. From S_E and Eq. (3), frequencies are computed and the fault components may be searched around them, as it is shown in Fig. 7. In order to avoid detecting peaks due to perturbations, components must be symmetrically placed from the fundamental frequency, and with similar modules.

Once these preliminary computations are done, a severity factor for the rotor (S_{RF}) is computed from expression (4). Then to obtain a final diagnosis, the CMS resorts to some expertise coded in a production system format, that is, a rule base. As it may be seen, the diagnostic system is

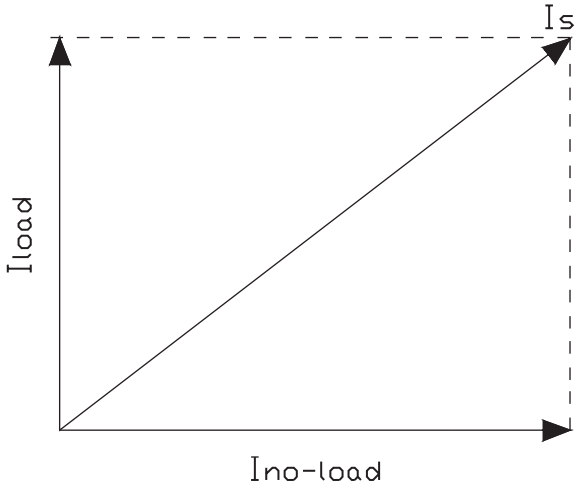

Fig. 5. Load percentage estimation.

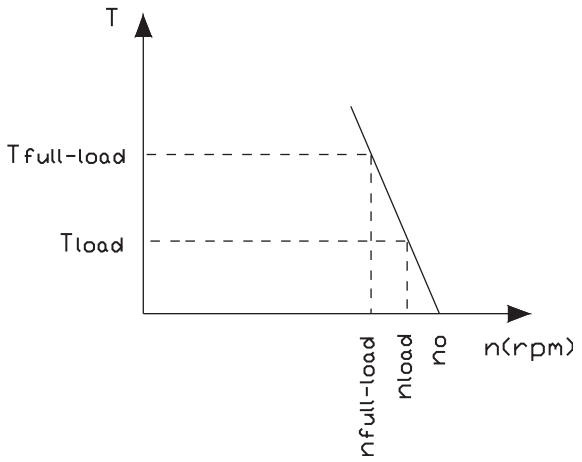

Fig. 6. Slip's estimation.

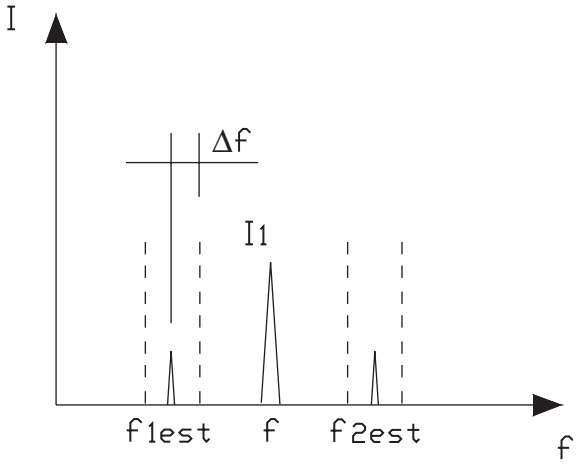

Fig. 7. Identification of the components of harmonic currents.

symptom driven and uses abduction to give an outcome [23]. In consequence, the working hypothesis for a successful diagnosis, is to consider a closed cause-symptoms universe, with every fault mode known beforehand. This strong assumption may be easily surpassed taking into account the unknown fault as a possible fault mode. Faults are then classified into "light", "moderate" and "strong". It was observed for the S_{SF} that normal induction motors have a value within 3%. Naturally, as the fault severity increases, the factor must also increase. Effectively, the fault discrimination in light, moderate and severe, was done based on the short circuit turn percentage in one phase. In order to be considered as a light fault, it shall allow the motor to keep on running without the need of an immediate stop. A moderate fault is the one producing overloads in the remaining phases, such that they push the motor to run in a risky mode. A severe fault, also produces current overload in the other phases, but in such a level that it causes risky

mechanical vibrations. The thresholds separating one kind of fault from another were determined from experimental observations.

In a normal running, the developed CMS may also give some warnings to improve the diagnosis, such as a repetition of the test with a higher/lower load level. As an example, one of these rules is presented next:

if $S_{SF} \geqslant 6.5\%$ *AND* $S_{SF} < 8\%$ *AND Load Factor* $\geqslant 0.5$

then

Fault : *one coil in short circuit* (*Moderate*)

Warning : *repeat diagnostic procedure with half the load for a better diagnosis.*

As regards the stator faults, the CMS computes the geometric locus of the PCV. Then its radius is decomposed in a Fourier series and a measure is done over the component with twice the supply frequency, as explained in Section 2.2. The severity factor (S_{SF}) is obtained from Eq. (9). Again, the knowledge base classifies the fault and may give hints to improve results.

4. Experimental results

4.1. The experimental prototype

The CMS proposed in this work consists of a data acquisition system sampling the stator currents from current transformers. The test bank is an induction motor dragging a direct current generator with variable load. The acquisition and human-machine interface tasks were developed with LabView. In Fig. 8 there is a schematic diagram, and in Fig. 9, a snapshot of the experimental prototype is used in this research.

The motor under diagnosis for these tests consists of an induction motor of 6 poles and 50 Hz that allows changing rotors with a different number of broken bars and access to diverse points of the stator winding.

4.2. Case study 1

Two broken bars in rotor and normal stator. The CMS estimates a 65% motor load, the motor speed yielded 989 rpm, and the slip was of 0.011. As a consequence of this, the frequencies to look for rotor faults were 48.9 and 51.1 rpm, using Eq. (3). Then the system searches for maximum in a range near these frequencies, verifying they are approximately at the same distance from the fundamental component. Components of -140.9 dB at 49.0 Hz and of -119.4 dB at 50.9 Hz, were found. As the load factor is between 50 and 75 (%), and the amplitude of these components was in the range from -100 to -150 dB, the rule base states that "*There is a moderate fault in rotor*" and gave a warning "repeat diagnostic procedure with a higher load for a better diagnosis". Also the CMS computed the stator current components among D and Q axes and obtained the frequency spectrum of Park's vector. It rises an average component of 5.93 A and a component of 0.12 A at 100 Hz. With these data, the S_{SF} using Eq. (9) results 2.02%. As this is smaller than the tolerance threshold of 3%, the CMS gave an outcome of "*No faults observed in the stator*".

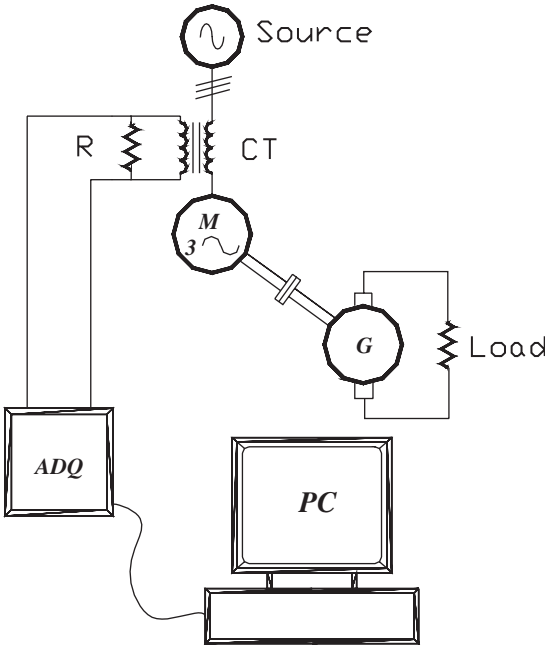

Fig. 8. A diagram of the experimental prototype.

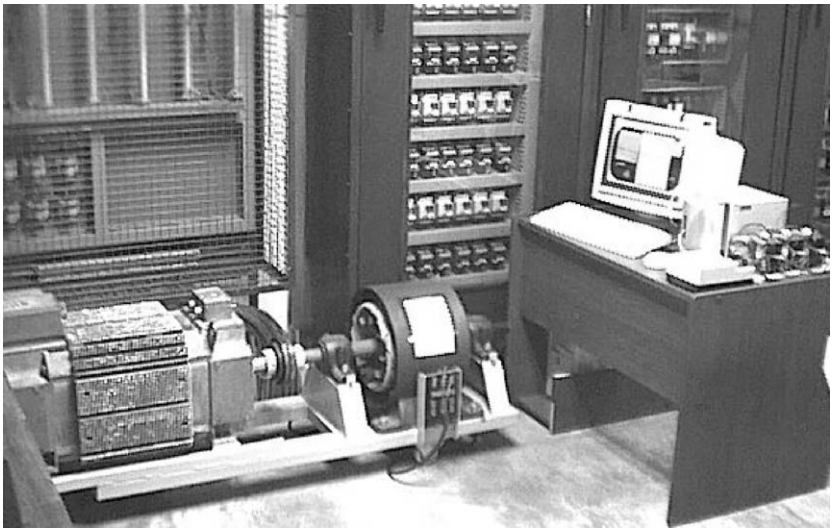

Fig. 9. A snapshot of the experimental prototype.

4.3. Case study 2

Three broken bars in rotor and normal stator. The CMS acquisition performance may be seen in Fig. 10. The load factor was estimated in 0.93% and the frequencies to look for faults were set using Eq. (1). As the motor is near its nominal charge the outcome for this case was "*There is a*

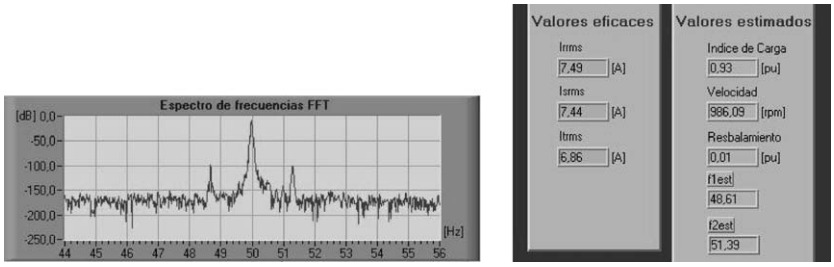

Fig. 10. Results from CMS for case study 2.

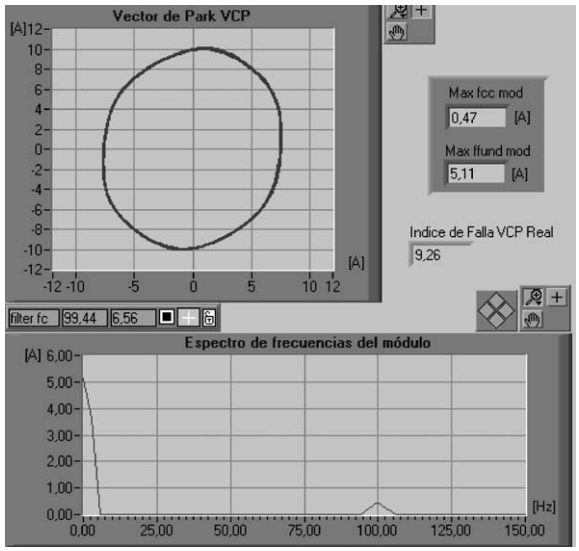

Fig. 11. Results from CMS for case study 3.

strong fault in rotor''. In Fig. 10 harmonic components due to faults were highlighted using a logarithmic scale. The CMS also states that ''*No faults observed in the stator*''. In effect, for the stator, the S_{SF} is less than 3%, which is considered as normal.

4.4. Case study 3

Normal rotor and short circuit in 12% of stator coils in one phase. The CMS's human–machine interface, consisting of the Park's Current Vector depicted and its decomposition in Fourier's series with diagnostic information, is shown in Fig. 11. The S_{SF} was 3.2% with the induction motor running without load and the knowledge base inference was ''*There is a light fault in stator*''. The CMS also reported ''*No faults observed in the rotor*''. In this last case, the S_{SR} could not be computed because the amplitude of stator current sidebands are small enough to be confused with the ripple in the acquired signal.

Table 1
Laboratory tests of CMS with the prototype of Fig. 10

Number of cases	Correct diagnosis	Incorrect diagnosis	Unknown diagnosis
25	21	3	1

4.5. General comments

It is important to take into account that the computed fault indexes may have a value different to zero even with new and without fault motors, as explained in Section 3. This is because the motor may have little abnormalities in construction (obviously depending on its quality control), and also because of unbalanced supply network, internal errors in sensors, quantification error, and others. Then, in order to avoid false positives when diagnosing, a special attention must be given to detect the threshold determination. The performance of the whole system will depend on threshold selection and tuning.

Beyond the presented case studies, several laboratory tests were done over the CMS with this experimental prototype, and obtained results are shown in Table 1. These tests were done with different kind of faults, different degrees of severity and with the motor in different operating points.

Another important hint to remark, from these great deal of laboratory tests, is that while the S_{SF} factor reflects the supply network unbalances, the S_{RF} factor, does not.

5. Conclusions

Based on several techniques for fault detection and diagnosis of induction machines proposed in the literature, the ones considered most promising were selected. The selection criteria were: non-invasive technique, minimum number of measured variables, discrimination power, and prior motor information to yield a diagnosis.

The obtained CMS gives general conclusions about the motor state, in a user-friendly interface. It was easily developed in Lab with commercial products. The added feature of a knowledge base confers the possibility of considering sensors fault or even unbalances in the supply network, as well as a qualitative classification of faults in light, moderate and strong. In cases of insufficient motor load, the system is able to recommend a warning for a better measure.

References

[1] D.J. Siyambalapitiya, P.G. MClaren, Reliability improvement and economic benefits of on-line monitoring system for large induction machines, IEEE Transactions on Industry Applications 26 (1990) 1018–1025.
[2] O.V. Thorsen, M. Dalva, A survey of faults on induction motors in offshore oil industry, petrochemical industry, gas terminals, and oil refineries, IEEE Transactions on Industry Applications 31 (1995) 1186–1196.

[3] A. Bonnett y, G. Soukup, Cause and analysis of stator ans rotor failures in three-phase squirrel-cage induction motors, IEEE Transactions on Industry Applications 28 (4) (1992) 921–937.
[4] S. Nandi, H. Toliyat, Fault diagnosis of electrical machines–a review. IEEE IEMCD'99, International Electric Machines and Drives Conference, May 9–12, Washington, USA, 1999.
[5] D.F. Busse, J.M. Erdman, R.J. Kerkman, D.W. Schlegel, G.L. Skibinski, The effects of PWM voltage source inverter on the mechanical performence of rolling bearings, IEEE Transactions on Industry Applications 33 (2) (1997) 567–576.
[6] M. Kaufhold, H. Auinger, M. Berth, J. Speck, M. Eberhardt, Electrical stress and failure mechanism of the winding insulation in PWM-Inverter-Fed low-voltage induction motors, IEEE Transactions on Industrial Electronics 47 (2) (2000) 396–402.
[7] G.B. Kliman, R.A. Koegl, J. Stein, R.D. Endicott, M.W. Madden, Noninvasive detection of broken rotor bars in operating induction motors, IEEE Transactions on Energy Conversion EC-3 (4) (1988) 873–879.
[8] J.R. Cameron, W.T. Thomson, A.B. Dow, Vibration and current monitoring for detecting airgap eccentricity in large induction motors, IEE Proceedings 133 (pt. B, 3) (1986) 155–163.
[9] D.G. Dorrell, W.T. Thomson, S. Roach, Analysis of airgap flux, current, and vibration signals as a function of the combination of static and dynamic airgap eccentricity in 3-phase induction motors, IEEE Transactions on Industry Applications 33 (1) (1997) 24–34.
[10] R. Schoen, B. Lin, T. Habetler, J. Schlag y, S. Farag, An unsupervised, on-line system for induction motor fault detection using stator current monitoring, IEEE Transactions on Industry Applications 31 (6) (1995) 1280–1286.
[11] S. Nandi, R. Bharadwaj, H.A. Toliyat, A.G. Parlos, Performance analysis of a three phase induction motor under mixed eccentricity condition, IEEE Power Electronic Drives and Energy Systems for Industrial Growth Conference Proceedings, 1998 International Conference, vol. 1, pp. 123–128.
[12] S.M.C. Cruz, A.J.M. Cardoso, Stator winding fault diagnosis in three-phase synchronous and asynchronous motors by the extended park's vector approach, Conference Record of the 2000 IEEE Industry Applications Conference, CD-ROM, Roma, Italy, October 2000, 7pp.
[13] H. Nejjari, M. Benbouzid, Monitoring and diagnosis of induction motors electrical faults using a current park's vector pattern learning approach, IEEE Transaction on Industry Applications 36 (3) (2000) 730–735.
[14] G. Salles, F. Filippetti, C. Tassoni, G. Grellet, G. Franceschini, Monitoring of induction motor load by neural network techniques, IEEE Transactions on Power Electronics 15 (4) (2000) 762–768.
[15] F. Filippetti, G. Franceschini, C. Tassoni, P. Vas, Recent developments of induction motor drives fault duagnosis using AI techniques, IEEE Transactions on Industrial Electronics 47 (5) (2000) 994–1004.
[16] P.V. Goode, M. Chow, Using a neural/fuzzy system to extract heuristic knowledge of incipient faults in induction motors, IEEE Transactions on Industrial Electronics 42 (2) (1995) 131–146.
[17] G. Acosta, C. Alonso, B. Pulido, Basic tasks for knowledge based supervision in process control, Engineering Applications of Artificial Intelligence 14 (4) (2001) 441–455 Elsevier Science Ltd/IFAC.
[18] F. Filippetti, G. Franceschini, C. Tassoni, P. Vas, AI techniques in induction machines diagnosis including the speed ripple effect, IEEE Transactions on Industry Applications 34 (1) (1998) 98–108.
[19] P. Krause, Analysis of Electric Machinery, McGraw-Hill Book Company, New York, 1986, pp. 164–210.
[20] W.T. Thomson, M. Fenger, Current signature analysis to detect induction motor faults, IEEE Industry Applications Magazine, July/August 2001, pp. 26–34.
[21] S.M.A. Cruz, A.J.M. Cardoso, Diagnóstico de Avarias no Rotor de Motores de Indução Trifásicos, 5° Congesso Nacional de Manutenção Industrial, Figueira da Foz, Portugal, Tema G, Comunicação (No 19), October 23–25, 1996.
[22] R. Schoen, T. Habetler, Effects of time-varying loads on rotor fault detection in induction machines, IEEE Transactions on Industry Applications 31 (4) (1995) 900–906.
[23] D. Poole, Normality and faults in logic-based diagnosis, in: Readings in Model Based Diagnosis, Morgan-Kaufmann Pub., Los Altos, CA, 1992, pp. 71–77.